A Complex Web of Signal-dependent Trafficking Underlies the Triorganellar Distribution of P-Selectin in Neuroendocrine PC12 Cells

Anastasiya D. Blagoveshchenskaya, Eric W. Hewitt, and Daniel F. Cutler

MRC Laboratory for Molecular Cell Biology, and Department of Biochemistry and Molecular Biology, University College London, London WC1E 6BT, United Kingdom

Abstract. By analyzing the trafficking of HRP–P-selectin chimeras in which the lumenal domain of P-selectin was replaced with horseradish peroxidase, we determined the sequences needed for targeting to synaptic-like microvesicles (SLMV), dense core granules (DCG), and lysosomes in neuroendocrine PC12 cells. Within the cytoplasmic domain of P-selectin, Tyr777 is needed for the appearance of P-selectin in immature and mature DCG, as well as for targeting to SLMV. The latter destination also requires additional sequences (Leu768 and ^{786}DPSP^{789}) which are responsible for movement through endosomes en route to the SLMV. Leu768 also mediates transfer from early transferrin (Trn)-positive endosomes to the lysosomes; i.e., operates as a lysosomal targeting signal. Furthermore, SLMV targeting of HRP–P-selectin chimeras, but not the endogenous SLMV protein synaptophysin/p38, previously shown to be delivered to SLMV directly from the plasma membrane, is a Brefeldin A–sensitive process. Together, these data are consistent with a model of SLMV biogenesis which involves an endosomal intermediate in PC12 cells. In addition, we have discovered that impairment of SLMV or DCG targeting results in a concomitant increase in lysosomal delivery, illustrating the entwined relationships between routes leading to regulated secretory organelles (RSO) and to lysosomes.

Key words: P-selectin • PC12 cells • lysosomes • dense core granules • synaptic-like microvesicles

Neuroendocrine cell lines have served as good model systems for studying the biogenesis of regulated secretory organelles (RSO)[1], i.e., the dense core granules (DCG) and synaptic-like microvesicles (SLMV), which are involved in storage and exocytotic release of soluble material after external stimulation. Although substantial progress has been made towards understanding trafficking routes to individual RSO, the relationships between routes to the different RSO, as well as between RSO and other post-Golgi destinations such as the lysosome, are largely unknown. Since more than one pathway contributes to the steady state intracellular distribution of many proteins, it is important to establish how paths leading to different destinations are interconnected and therefore how homeostasis of RSO membrane composition is maintained. This is especially important for membrane proteins that are found in both RSO such as vesicle-associated membrane protein (VAMP) I and II, as well as synaptotagmin I (Elferink et al., 1993; Walch-Solimena et al., 1993; Chilcote et al., 1995; Papini et al., 1995).

An extreme example of a multiorganellar distribution is that exhibited by P-selectin. This type I membrane protein was originally found in the specialized secretory granules of endothelial cells and platelets (Bonfanti et al., 1989; McEver et al., 1989). It belongs to a family of adhesion molecules and operates in early stages of the inflammatory response as a receptor for leukocytes (Johnston et al., 1989). When expressed in nonendothelial cells, P-selectin is sorted to secretory granules and/or constitutively delivered to the cell surface (Disdier et al., 1992; Koedam et al., 1992; Subramaniam et al., 1993; Setiadi et al., 1995). From the plasma membrane, P-selectin is rapidly internalized to endosomes and then, depending on the cell type, either recycles back to secretory granules (Koedam et al., 1992; Subramaniam et al., 1993) or is delivered to SLMV (Strasser et al., 1999, in press) or to lysosomes for degradation (Green et al., 1994; Blagoveshchenskaya et al., 1998a,b; Straley et al., 1998). Interestingly, despite its effi-

Address all correspondence to Daniel F. Cutler, MRC Laboratory for Molecular Cell Biology, and Department of Biochemistry and Molecular Biology, University College London, Gower Street, London WC1E 6BT, United Kingdom. Tel.: 44-171-380-7808. Fax: 44-171-380-7805. E-mail: d.cutler@ucl.ac.uk

1. *Abbreviations used in this paper:* AP, adaptor protein; ARF1, adenosine ribosylation factor 1; BFA, Brefeldin A; DCG, dense core granules; iDCG, immature dense core granules; mDCG, mature dense core granules; GTI, granule targeting index; HB, homogenization buffer; LTI, lysosomal targeting index; NAGA, *N*-acetyl-β-D-glucosaminidase; RSO, regulated secretory organelles; SLMV, synaptic-like microvesicles; SLMV-TI, SLMV targeting index; SSV, small synaptic vesicles; Trn, transferrin; TrnR, Trn receptor; VAMP, vesicle-associated membrane protein.

cient endocytosis, no discrete internalization signal has been found within this protein (Setiadi et al., 1995).

The cytoplasmic tail of P-selectin has been found to be both necessary and sufficient for mediating the delivery of this protein to different post-Golgi destinations, i.e., DCG and SLMV, and lysosomes, although the transmembrane domain of P-selectin was recently shown to increase the efficiency of granule targeting (Fleming et al., 1998). Together, these findings suggest that P-selectin provides an ideal model with which to examine the relations between different post-Golgi pathways taken by the same protein.

Among neuroendocrine cell lines, PC12 is the best characterized with respect to both RSO, SLMV and DCG. SLMV are considered to be a neuroendocrine counterpart of the small synaptic vesicles (SSV) from neurons, since they share many biochemical and physical properties with authentic SSV (Clift-O'Grady et al., 1990). The DCG are the dominant RSO in endocrine cells and they store and release not only classical neurotransmitters, but also peptides and proteins (Cramer and Cutler, 1992; Bauerfeind and Huttner, 1993). When expressed in PC12 cells, P-selectin is targeted to both RSO as well as to lysosomes, thus providing a highly appropriate system to investigate relationships between these different trafficking routes.

One complication in carrying out this sort of analysis is that there is often more than one route to organelles. For example, although there is a consensus as to the initial step of SLMV/SSV formation which involves the constitutive delivery of newly synthesized SLMV membrane proteins from the TGN to the plasma membrane (Cutler and Cramer, 1990; Regnier-Vigouroux et al., 1991; Bauerfeind and Huttner, 1993), subsequent trafficking from the plasma membrane to the SLMV/SSV remains less clear, with two alternative routes being proposed, one direct from the plasma membrane and another involving an endosomal intermediate.

In contrast, DCG bud from the TGN. Newly formed granules (immature DCG, iDCG) are often partially coated with clathrin and adaptor protein (AP) 1, which are involved in a remodelling process leading to mature DCG (mDCG) which are devoid of coats (Arvan and Castle, 1998; Tooze, 1998). A direct route incorporating newly synthesized DCG membrane proteins into forming iDCG from the TGN would therefore be expected to operate, although evidence for this process is currently lacking. In addition, resident granule membrane proteins are capable of recycling to granules via the plasma membrane, endosomal intermediates, and the TGN (Patzak and Winkler, 1986; von Grafenstein and Knight, 1992; Partoens et al., 1998).

The third major destination of P-selectin is the lysosome. A substantial body of data has established that membrane proteins are delivered to lysosomes by two routes, either directly from the TGN via endosomes or via the plasma membrane followed by a passage through endosomal compartments en route to lysosomes (Kornfeld and Mellman, 1989; Hunziker and Geuze, 1996).

Given such a multiplicity of post-Golgi routes, how might a complex distribution such as the triorganellar localization shown by P-selectin be achieved? An accumulating body of evidence indicates that trafficking of transmembrane proteins to post-Golgi destinations is controlled by short, specific sequences (often called targeting signals) located in their cytoplasmic domains. The most common targeting signals are classified into two groups, tyrosine- and dileucine-based signals. The signals mediating lysosomal targeting generally belong to these two families, although novel categories of lysosomal targeting signals (LTS) have recently been described (Subtil et al., 1997; Blagoveshchenskaya et al., 1998a,b; Straley et al., 1998).

Some targeting signals have been shown to mediate more than one sorting step, e.g., those controlling internalization from the plasma membrane and subsequent trafficking to lysosomes, or endocytosis and trafficking to SLMV (Sandoval and Bakke, 1994; Grote et al., 1995; Grote and Kelly, 1996; Marks et al., 1997). Given the endosomal origin of SLMV documented by some investigators, the targeting requirements for delivery to SLMV and lysosomes might overlap. However, there is no experimental support for this notion, since resident SLMV proteins have not been thought to be targeted to lysosomes. Moreover, whether common signals are used for delivery to the two different RSO is not yet clear either, although data on VAMPII expressed in insulinoma cells suggest that targeting requirements to both RSO might be similar (Regazzi et al., 1996). Nevertheless, despite the numerous studies of sequence requirements mediating post-Golgi trafficking, analyses of multiorganellar targeting of single proteins have not been attempted.

In this study, we examined the signal dependence of targeting to three major post-Golgi destinations in PC12 cells, SLMV, DCG, and lysosomes, by following HRP–P-selectin chimeras in which the extralumenal domain of P-selectin was replaced with HRP. These chimeras provide a quantitative and convenient enzymatic assay with which to detect the protein in a variety of intracellular compartments (Connolly et al., 1994; Stinchcombe et al., 1995; Norcott et al., 1996; Blagoveshchenskaya et al., 1998a,b; Strasser et al., 1999). Here, we describe how the complex distribution of P-selectin is controlled by multiple determinants, some of which are needed for more than one destination. The pattern of usage of the targeting determinants reveals relationships between the pathways leading to the three organelles. In addition, our data determine the extent of the contribution of different routes to the target organelles. Finally, the pattern of changes in distribution of P-selectin to these organelles, when one or two destinations are removed from the protein's itinerary, shows how post-Golgi trafficking choices are restricted.

Materials and Methods

Materials and Reagents

Mouse monoclonal (clone 2H11) and rabbit polyclonal anti-HRPs were purchased from Advanced ImmunoChemical Inc. and from DAKO, respectively. Polyclonal antibodies against secretogranin II and synaptophysin/p38 have been described previously (Cutler and Cramer, 1990). Immobilon-P membrane was obtained from Millipore; ^{3}H-Dopamine was from Amersham International; NHS-SS-biotin was from Pierce; Express ^{35}S-labeling mix of methionine and cysteine was from NEN Life Science Products; and Amplify™ was from Amersham. Other chemicals were purchased from Sigma Chemical Co.

Mouse receptor grade epidermal growth factor (EGF), human iron saturated transferrin (Trn), protein A, and 2H11 were iodinated using the modified IODO-GEN procedure as described elsewhere (Wiley and Cunningham, 1982).

Constructs

A chimeric cDNA comprising the human growth hormone signal sequence followed by HRP, the transmembrane domain, and cytoplasmic tail of P-selectin (see Fig. 2) was generated as previously described (Norcott et al., 1996), as were chimeras with deletions of the cytoplasmic tail. The tetra-alanine substitutions and point mutations were made as described (Blagoveshchenskaya et al., 1998a,b). Two additional mutants were constructed in the same way using the following primers: Y777A: AGCCACCTAGGAACAGCTGGAGTTTTTACAAA and Y777F: AGCCACCTAGGAACATTTGGAGTTTTTACAAA. Only the sense primer is shown, the anti-sense primer used is the exact complement. The constructs obtained were confirmed by sequencing.

Cell Culture and Transfection

The rat pheochromocytoma cell line PC12 (CCL23; American Type Culture Collection) was maintained and transfected as described previously (Norcott et al., 1996). Where necessary, cells were stimulated with 10 mM Carbachol for 30 min at 37°C.

Endocytosis of External Ligands and ^{3}H-Dopamine Labeling

Cells were labeled with ^{125}I-Trn or ^{125}I-EGF as described previously (Blagoveshchenskaya et al., 1998a). Removal of cell surface–bound ligands was as described in Blagoveshchenskaya et al. (1998a). ^{125}I-2H11 (1 μg/ml) was internalized for 1 h at 37°C in growth medium and then cells were placed on ice. Antibody present on the plasma membrane was removed by treatment of cells with acidic buffer (100 mM sodium acetate, pH 4.0, and 500 mM NaCl) on ice twice for 10 min each. DCG were labeled with ^{3}H-Dopamine as previously described (Norcott et al., 1996).

Pulse–Chase Metabolic Labeling Experiments

PC12 cells grown on 150-mm dishes to 70% confluency were rinsed twice with methionine/cysteine-free DME supplemented with 0.5% FCS and cultivated in this medium for 30 min in the CO_2-incubator. Cells were pulsed in 15 ml of methionine/cysteine-free DME containing 2 mCi of Express ^{35}S-labeling mix and 1% FCS for 10 min at 37°C, washed with growth medium, and chased for either 20 min at 37°C or 16 h at 37°C in fresh growth medium. ^{35}S-labeled cells were washed three times with ice-cold HSE buffer (0.25 M sucrose, 10 mM Hepes-KOH, pH 7.2, 1 mM EDTA, 2 mM PMSF, 10 μg/ml aprotinin, 10 μg/ml leupeptin, and 10 μg/ml pepstatin A) and subjected to subcellular fractionation for isolation of immature and mature DCG (see below).

Subcellular Fractionation and Quantitation of Data

Subcellular fractionation of PNS on the initial 1–16% Ficoll velocity gradients, secondary 5–25% Ficoll velocity gradients for lysosome isolation and 5–25% Glycerol velocity gradients for SLMV isolation were carried out as described (Norcott et al., 1996; Blagoveshchenskaya et al., 1998a)

Calculation of Lysosomal Targeting Indexes and SLMV Targeting Indexes. Cells were fed with ^{125}I-2H11 as described above, homogenized, and then subjected to a two-stage fractionation procedure for lysosomal isolation. Targeting data were presented as a lysosomal targeting index (LTI), i.e., the amount of ^{125}I-2H11 radioactivity present in the lysosomal peak for each chimera normalized to that for wild-type ssHRP$^{P\text{-selectin}}$. In all experiments, the LTI for wild-type ssHRP$^{P\text{-selectin}}$ was set at 1. To take into account variations of expression level and lysosomal yield, the amount of ^{125}I-2H11 radioactivity present in the lysosomal peak (^{125}I-2H11 peak) has been corrected for the amount of NAGA activity (NAGA peak) within the lysosomal fractions and for total ^{125}I-2H11 radioactivity in the homogenate (^{125}I-2H11 hmg). After simplifying the original equation, the LTI was defined as follows:

$$\mathrm{LTI} = \frac{\dfrac{\text{mutant } ^{125}\text{I-2H11 peak}}{\text{mutant } ^{125}\text{I-2H11 hmg}} : \dfrac{\text{mutant NAGApeak}}{\text{mutant NAGA hmg}}}{\dfrac{\text{WT } ^{125}\text{I-2H11 peak}}{\text{WT } ^{125}\text{I-2H11 hmg}} : \dfrac{\text{WT NAGApeak}}{\text{WT NAGAhmg}}}. \quad (1)$$

Typically, the LTI for tail-less ssHRP$^{P\text{-selectin763}}$ was subtracted from those for the other chimeras in each experiment to provide a baseline, i.e., the LTI for ssHRP$^{P\text{-selectin763}}$ was considered as 0. The LTIs of the mutants were therefore described on a scale within a range set by ssHRP$^{P\text{-selectin}}$ (1) and ssHRP$^{P\text{-selectin763}}$ (0).

SLMV targeting indexes were calculated by normalizing the amount of HRP activity in the peak (see Fig. 5) for synaptophysin (p38) recovery and chimera expression level as indicated below. Amounts of p38 in the SLMV peaks and in the homogenate were determined by quantitative Western blotting as described (Blagoveshchenskaya et al., 1998b).

$$\text{SLMV-TI} = \frac{\dfrac{\text{mutant HRP peak}}{\text{mutant HRP hmg}} : \dfrac{\text{mutant p38 peak}}{\text{mutant p38 hmg}}}{\dfrac{\text{WT HRP peak}}{\text{WT HRP hmg}} : \dfrac{\text{WT p38 peak}}{\text{WT p38 hmg}}}. \quad (2)$$

Secondary Sucrose Equilibrium Gradients for Separation of Late Endosomes and DCG. Those fractions (14–20) from initial 1–16% Ficoll gradients containing most ^{3}H-Dopamine radioactivity were pooled, diluted with HB (320 mM sucrose, 10 mM Hepes-NaOH, pH 7.3), and 4 ml of this material was then layered on top of 9 ml preformed 0.9–1.85 M sucrose gradients. The gradients were centrifuged at 35,000 rpm for 20 h in a SW40Ti rotor and fractionated. The lighter peak of HRP activity containing NAGA and internalized ^{125}I-EGF corresponds to late endosomes, while the denser peak, which overlaps with ^{3}H-Dopamine distribution, contains the DCG (see Fig. 1 B).

To quantitate targeting to DCG, granule targeting indexes (GTI) were calculated essentially as described above, except ^{3}H-Dopamine was used to normalize for DCG recovery as follows:

$$\mathrm{GTI} = \frac{\dfrac{\text{mutant HRP peak}}{\text{mutant HRP hmg}} : \dfrac{\text{mutant } ^3\text{H peak}}{\text{mutant } ^3\text{H hmg}}}{\dfrac{\text{WT HRP peak}}{\text{WT HRP hmg}} : \dfrac{\text{WT } ^3\text{H peak}}{\text{WT } ^3\text{H hmg}}}. \quad (3)$$

Initial 0.3–1.2 M Sucrose Velocity Gradients for Isolation of iDCG and mDCG. The gradient system used was that established earlier by Tooze and Huttner (1990) and then modified (Dittie et al., 1997). In brief, after three washes with ice-cold HSE buffer, cells from one 150-mm dish were scraped in this buffer and pelleted by low-speed centrifugation at 1,000 *g* for 3 min. The supernatant was discarded and cells resuspended in 2 ml of fresh HSE buffer were then passed 10 times through a ball bearing homogenizer with 0.01-mm clearance. After centrifugation of the homogenate at 1,000 *g* for 10 min, 1.3 ml of PNS was layered on top of an 11-ml preformed 0.3–1.2 M sucrose gradient made in 10 mM Hepes-KOH, pH 7.2, and centrifuged in a SW40Ti rotor for 19 min with slow acceleration and deceleration. The gradients were then collected in 1-ml fractions from the top of the tube.

Secondary 0.9–1.7 M Sucrose Equilibrium Gradients for Isolation of iDCG and mDCG. After fractionation of the initial 0.3–1.2 M sucrose gradients, the fractions containing iDCG (fractions 2–4) or mDCG (fractions 4–6) (Dittie et al., 1997) were pooled, diluted with 10 mM Hepes-KOH, pH 7.2, to a final volume of 4 ml, and then layered on top of 9-ml preformed 0.9–1.7 M sucrose gradients made in 10 mM Hepes-KOH, pH 7.2, and recentrifuged to equilibrium for 21 h in a SW40Ti rotor. 1-ml fractions were collected from the top of the equilibrium gradients. 200 μl of each fraction was diluted in NDET buffer to 10 ml (final concentration: 1% NP-40, 0.4% sodium deoxycholate, 66 mM EDTA, 10 mM Tris-HCl, pH 7.4, 1 mM PMSF, 10 μg/ml aprotinin, 10 μg/ml leupeptin, and 10 μg/ml pepstatin A) and used for immunoprecipitation of ^{35}S-labeled SgII. The rest was aliquoted and used for measurement of HRP activity or for Western blotting with anti-SgII.

Immunoprecipitation, Fluorography, and Quantitation of Data

Immunoprecipitation using polyclonal anti-SgII followed by SDS-PAGE was carried out as described previously (Cramer and Cutler, 1992). The gels were exposed to a PhosphorImager screen for weak β emission (Bio-Rad Laboratories) and then to x-ray film for 2 d. Quantitation of data was performed using Molecular Analyst software (Bio-Rad Laboratories). The distribution of unlabeled SgII across the gradients was analyzed by Western blots of fractions followed by detection with polyclonal anti-SgII, then with ^{125}I–protein A and PhosphorImager exposure.

Miscellaneous Methods

N-acetyl-β-D-glucosaminidase activity was determined as described (Kornilova et al., 1992). Protein concentration was measured using the Micro

BCA protein assay kit (Pierce) according to the manufacturer's instructions. HRP activity in the samples was determined in triplicate as previously described (Norcott et al., 1996). HRP proteolysis, internalization assays, and the DAB cytochemistry were carried out as described (Blagoveshchenskaya et al., 1998a,b).

Results

A New Two-Step Subcellular Fractionation Procedure for Separation of DCG and Late Endosomes

We set out to reexamine the determinants needed for DCG targeting of P-selectin in PC12 cells where parallel analyses of SLMV and lysosomal targeting were being carried out. To quantitatively evaluate targeting of HRP–P-selectin chimeras (see Fig. 2) to DCG at steady state conditions, we have introduced an improved subcellular fractionation protocol for DCG isolation, as illustrated in Fig. 1, because of the contamination of DCG enriched fractions by late endosomes.

The first stage of DCG isolation is a velocity centrifugation of PNS on preformed linear 1–16% Ficoll gradients as described earlier (Cramer and Cutler, 1992; Norcott et al., 1996). This procedure was originally developed to separate SLMV and DCG, but has also proved successful for the separation of plasma membrane, multiple endosomal compartments, and lysosomes (Blagoveshchenskaya et al., 1998a). To determine the position of intracellular compartments on this gradient, the distributions of ^{125}I-Trn (early recycling endosomes), ^{125}I-EGF (late endosomes), ^{3}H-Dopamine (DCG), and NAGA activity (lysosomes) were monitored. PC12 cells transfected so as to transiently express ssHRP$^{P\text{-selectin}}$ were loaded either with ^{3}H-Dopamine, ^{125}I-Trn, or ^{125}I-EGF, homogenized, and a PNS was then centrifuged on linear 1–16% Ficoll gradients. The early endosomes containing ^{125}I-Trn sedimented in the low density fractions 5–10 (Figs. 1 A and 9). After binding to the plasma membrane at 4°C, ^{125}I-EGF was allowed to internalize for 20 min at 37°C to reach late endosomal compartments (Fig. 1 A). The distribution of ^{3}H-Dopamine overlaps both with ^{125}I-EGF and partially with NAGA in fractions 14–20 (Fig. 1 A), indicating that DCG and late endosomes have similar sedimentation characteristics under these centrifugation conditions.

To separate late endosomes from DCG, fractions containing the majority of ^{3}H-Dopamine radioactivity (14–20) (Fig. 1 A) were pooled and recentrifuged on 0.9–1.85 M sucrose gradients. The single peak of HRP activity seen on the initial Ficoll gradient (Fig. 1 A) splits into two peaks on the sucrose gradient (Fig. 1 B). The lighter peak of HRP activity corresponds to late endosomes since it cosediments with NAGA and ^{125}I-EGF internalized for 20 min at 37°C, but is devoid of ^{125}I-Trn. Although we have no direct evidence from these data as to whether the HRP activity is within the same organelles which contain NAGA and ^{125}I-EGF, we have used a diaminobenzidine density shift procedure to show that this is the case in H.Ep.2 cells (Blagoveshchenskaya et al., 1998a). The second, denser peak of HRP activity codistributes with the single peak of ^{3}H-Dopamine, thereby indicating the position of DCG on this gradient (Fig. 1 B). Therefore, to quantitate targeting to DCG for each chimera, we measured the amount of HRP activity within the latter peak.

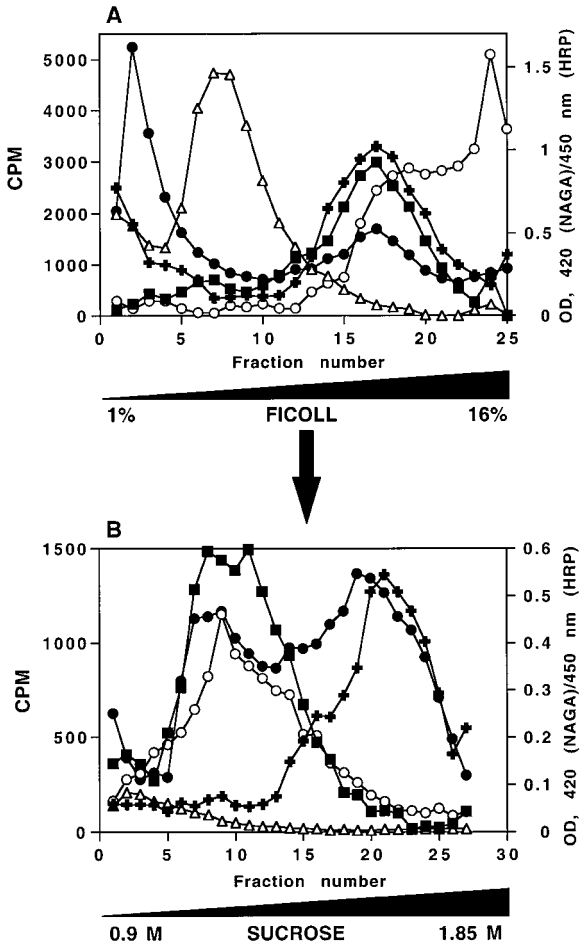

Figure 1. A two-step subcellular fractionation procedure for separation of late endosomes and DCG. (A) Distribution of intracellular compartments from PC12 cells on 1–16% Ficoll gradients. PC12 cells expressing ssHRP$^{P\text{-selectin}}$ were loaded with ^{3}H-Dopamine, or labeled with ^{125}I-Trn or^{125}I-EGF as described in Materials and Methods. Cells were homogenized in HB and the PNS was centrifuged on 1–16% Ficoll gradients and fractionated. The early/recycling endosomes are shown by the distribution of ^{125}I-Trn endocytosed for 60 min at 37°C (△). Late endosomes are shown by the distribution of ^{125}I-EGF internalized for 20 min at 37°C (■). The distribution of NAGA activity ($OD_{420\,nm}$; ○), HRP activity ($OD_{450\,nm}$; ■) and ^{3}H-Dopamine radioactivity (filled plus signs) along 1–16% Ficoll gradients are shown. (B) Separation of DCG and late endosomes on a secondary 0.9–1.85 M sucrose gradient. Fractions 14–20 from the 1–16% Ficoll gradients were pooled, diluted with HB, and recentrifuged on 0.9–1.85 M sucrose gradients to equilibrium. The distributions of NAGA activity (○), HRP activity (●), ^{3}H-Dopamine radioactivity (filled plus signs),^{125}I-EGF internalized for 20 min at 37°C (■) and ^{125}I-Trn (△) after centrifugation on this gradient are shown.

The Sequences YGVF and TNAAF, Located within the C2 Domain of the Cytoplasmic Tail, Are Necessary for Targeting of HRP–P-Selectin Chimeras to DCG

We have carried out a screen for short discrete determinants in the cytoplasmic domain that might mediate trafficking to the DCG in PC12 cells, using a series of HRP–P-selectin chimeras (Fig. 2). Inclusion of the transmembrane

domain, as in these chimeras, has been recently shown to increase the efficiency of targeting to DCG in neuroendocrine RIN5 cells, presumably by providing a more native context in which the cytoplasmic domain operates (Fleming et al., 1998). Cells expressing HRP–P-selectin chimeras were loaded with ^{3}H-Dopamine, homogenized, and then the PNS was fractionated as described above. We have monitored the targeting efficiency for each chimera by calculating a granule targeting index (GTI). Most of the chimeras with tetrapeptide substitutions show GTI similar to that for ssHRP$^{P\text{-selectin}}$ (GTI = 1) (Fig. 3 B). However, targeting to granules of ssHRP$^{P\text{-selectinYGVF}}$ and ssHRP$^{P\text{-selectinTNAAF}}$ was reduced by ~85%: 0.12 ± 0.06 (± SE) and 0.172 ± 0.1, correspondingly (Fig. 3 B).

YGVF resembles a typical Tyr-based sorting signal conforming to the consensus YXXø (where X is any amino acid and ø is a bulky hydrophobic amino acid). Since Tyr is often a critical residue within such signals (Trowbridge et al., 1993; Sandoval and Bakke, 1994; Marks et al., 1997), we examined the contribution of Tyr777 to DCG targeting. As shown in Fig. 3 C, substitution of Tyr777 by Ala, but not by Phe, reduced the GTI by 79%, i.e., to the level

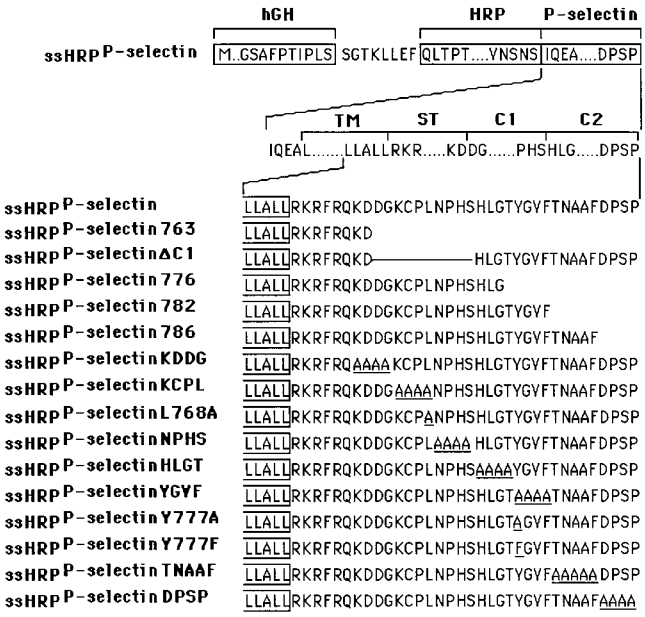

Figure 2. Schematic illustration of HRP–P-selectin chimeras. The top line shows the components used for construction: boxes represent the individual components; sequences outside boxes were added during construction. hGH, human growth hormone signal sequence; HRP, enzymatically active domain of HRP; P-selectin, transmembrane (TM); and cytoplasmic domains of P-selectin. The 35 residues of the wild-type cytoplasmic domain have been assigned to the stop transfer (ST), C1 and C2 domains according to exon–intron boundaries. The bottom part shows the full amino acid sequences of the cytoplasmic domains of the chimeras starting with the wild-type P-selectin tail, ssHRP$^{P\text{-selectin}}$. The carboxy-terminal end of the TM domain shown is boxed. The name of each chimera is listed to the left of the diagram. The number at the end of the name indicates the amino acid changed to a stop signal (numbering from the human P-selectin sequence). The tetrapeptide sequence(s) or number of a single amino acid at the end of each chimera's name show the residues that have been replaced by alanine.

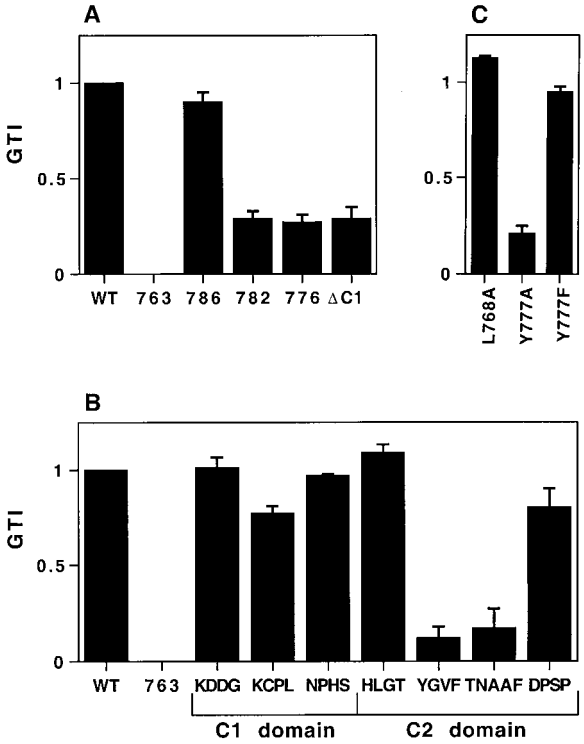

Figure 3. Targeting of HRP–P-selectin chimeras to DCG in PC12 cells. PC12 cells expressing the HRP–P-selectin chimeras shown in Fig. 2 were labeled with ^{3}H-Dopamine and fractionated as described in the legend for Fig. 1. Targeting to DCG was quantitated by calculating a GTI for each chimera. Each GTI is expressed on a scale related to the WT chimera (GTI = 1) and the tail-less chimera (GTI = 0). Each bar represents the mean ± SE of 3–10 independent determinations for each chimera. Deviations of <0.015 are not displayed. (A) GTIs for the deletion mutants; (B) GTIs for the tetra-alanine substitutions; (C) GTIs for the point mutations.

of ssHRP$^{P\text{-selectinYGVF}}$, while substitution of Phe780 by Ala did not cause a significant fall of the GTI. Therefore, Tyr777 makes a major contribution to the promotion of granule targeting but can be substituted by another aromatic amino acid without loss of function.

Substitution of the sequences surrounding YGVFTNAAF does not have a pronounced effect on DCG targeting. However, we have also tested the effects of grosser alterations within the C2 domain (Fig. 3 A). In agreement with the effect of tetrapeptide alanine substitutions (Fig. 3 B), removal of four carboxy-terminal amino acids (DPSP) did not affect the GTI (Fig. 3 A), whereas larger truncations including removal of TNAAF or TYGVFTNAAF reduced the GTI to levels similar to that of ssHRP$^{P\text{-selectinY777A}}$. Deleting the entire C1 domain also caused the GTI to fall, implying that the spacing between YGVFTNAAF and the lipid bilayer may be important for granule targeting in PC12 cells.

ssHRP$^{P\text{-selectin}}$ but Not ssHRP$^{P\text{-selectinY777A}}$ Is Found in both Immature and Mature DCG in PC12 Cells

Although we and others have shown that when expressed

in neuroendocrine cells, P-selectin is targeted to DCG (Disdier et al., 1992; Green et al., 1994; Norcott et al., 1996; Fleming et al., 1998; this paper), the distribution of this protein between iDCG and mDCG has not been determined, although current models for granule biogenesis (Arvan and Castle, 1998; Tooze, 1998) imply that any protein found within mDCG will first enter the iDCG from the TGN. It is of interest to determine whether a mutant that fails to accumulate in mDCG also fails to enter the iDCG (i.e., sorting occurs at the level of the TGN) or is found only in the precursor iDCG population (i.e., signal-mediated sorting is occurring during maturation of iDCG to mDCG). To address this issue, we have adopted a well-established subcellular fractionation procedure for separation of iDCG and mDCG (Tooze and Huttner, 1990; Tooze et al., 1991; Dittie et al., 1997). PC12 cells transiently expressing wild-type HRP$^{P\text{-selectin}}$ were pulsed and then chased to label iDCG or mDCG followed by fractionation as described (Materials and Methods). Fractions rich in iDCG or mDCG were collected and recentrifuged on 0.9–1.7 M sucrose equilibrium gradients followed by fractionation and immunoprecipitation with anti-secretogranin II (SgII, a soluble marker protein of DCG) and SDS-PAGE. The distribution on the secondary equilibrium gradient of ^{35}S-labeled SgII shows a clear separation of iDCG (Fig. 4 A) from mDCG (Fig. 4 B), with iDCG peaking in fractions 7–10 and mDCG in fractions 10–13. We wished to determine whether the HRP activity of wild-type ssHRP$^{P\text{-selectin}}$ is present within these peaks. Since, this analysis is performed at steady state conditions rather than in pulse–chase experiments, we first examined the steady state distribution along the gradients of the defining marker, SgII. Western blotting (Fig. 4, C and D) shows that even at steady state, SgII is found within those same peaks corresponding to iDCG and mDCG as revealed by pulse–chase experiments (Fig. 4, A and B).

To confirm that SgII is indeed present within functional secretory granules, we examined the effects of secretagogue stimulation on both peaks. In agreement with previous studies (Tooze and Huttner, 1990; Tooze et al., 1991), the peaks corresponding to both iDCG and mDCG diminished after carbachol treatment (Fig. 4, E and F). Having established the distribution of the secretagogue-responsive peaks of SgII corresponding to iDCG and mDCG, we determined the distribution of HRP–P-selectin chimeras on the same gradients. Accordingly, PC12 cells expressing ssHRP$^{P\text{-selectin}}$ were fractionated as above followed by measurement of HRP activity across the secondary equilibrium gradients. We have also analyzed the effect of secretagogue stimulation on distribution of HRP activity across these gradients. Fig. 4, G and H, show that ssHRP$^{P\text{-selectin}}$ is present within both iDCG (fractions 7–10) and mDCG (fractions 10–13) and that both peaks of HRP activity are responsive to secretagogue.

Since P-selectin has a more complex intracellular distribution than SgII, we expected that in addition to the DCG peaks, there would also be HRP activity corresponding to other organelles. Indeed, in addition to the peaks representing iDCG and mDCG, there is substantial HRP activity within a lighter peak (fractions 5 and 6; Fig. 4, G and H). However, unlike the fall of HRP activity within iDCG and mDCG, HRP activity in the lighter peak increases after secretagogue stimulation. Since secretagogue action transfers ssHRP$^{P\text{-selectin}}$ from the DCG to the plasma membrane and thence via endosomes to SLMV (Strasser et al., 1999), we presume that the material in fractions 5 and 6 represents a mixture of SLMV, plasma membrane, and endosomes.

Quantitation of HRP activity revealed that 7.2% of the ssHRP$^{P\text{-selectin}}$ in the homogenate was recovered within the

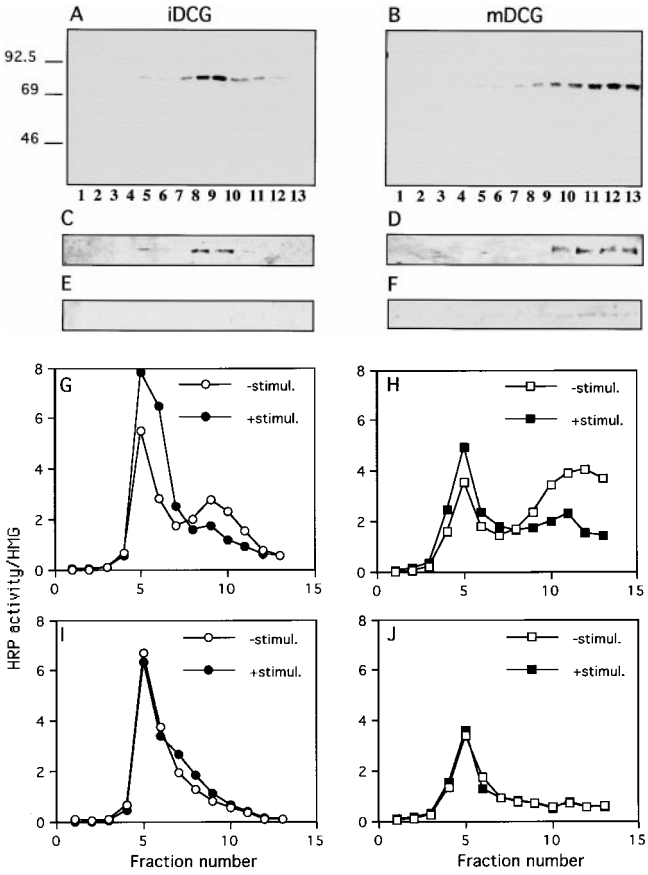

Figure 4. Sorting of SgII, ssHRP$^{P\text{-selectin}}$, and ssHRP$^{P\text{-selectinY777A}}$ to iDCG and mDCG. (A and B) PC12 cells expressing ssHRP$^{P\text{-selectin}}$ were pulsed for 10 min at 37°C with ^{35}S-labeling mix and chased for 20 min at 37°C (A) or for 16 h (B) at 37°C to label iDCG or mDCG, respectively. The PNS obtained from these cells was centrifuged on initial 0.3–1.2 M sucrose velocity gradients followed by recentrifugation of fractions corresponding to iDCG or mDCG on 0.9–1.7 M sucrose equilibrium gradients as described in Materials and Methods. After fractionation, 200 μl of each fraction was diluted with NDET buffer and immunoprecipitated with anti-SgII. The samples were then separated by 10% SDS-PAGE under reducing conditions, dried, and exposed to a PhosphorImager screen (Bio-Rad Laboratories). Alternatively, cells expressing ssHRP$^{P\text{-selectin}}$ (C–H) or ssHRP$^{P\text{-selectinY777A}}$ (I and J) were stimulated with 10 mM Carbachol for 30 min at 37°C (E, F, G ●, H ■, I ●, and J ■), or incubated without secretagogue (C, D, G ○, H □, I ○, and J □) and subjected to the two-step fractionation procedure for separation of iDCG and mDCG, as described in the legend for A and B. After fractionation, aliquots of each fraction were separated by SDS-PAGE followed by Western blotting using anti-SgII followed by ^{125}I–protein A (C–F) or used for measurement of HRP activity normalized to that in the homogenate (G–J).

iDCG, whereas 14% was present in the mDCG. Importantly, this ratio is comparable to that for SgII recovered at steady state conditions within the iDCG and mDCG, as judged by quantitative Western blotting, 10 and 28%, respectively. Thus, when expressed in PC12 cells, ssHRP$^{P\text{-}selectin}$ is found in the iDCG and mDCG in a ratio similar to that of the DCG marker protein SgII.

Having established that wild-type ssHRP$^{P\text{-}selectin}$ is sorted to both iDCG and mDCG, we determined whether a DCG targeting mutant is present in iDCG but not in mDCG, or whether it is found in neither population. Therefore, we have examined the targeting of ssHRP$^{P\text{-}selectinY777A}$ to both populations of DCG. After the fractionation of PNS obtained from cells expressing ssHRP$^{P\text{-}selectinY777A}$, no peaks of HRP activity within the fractions corresponding either to iDCG (fractions 7–10) or to mDCG (fractions 10–13) was detected (Fig. 4, I and J), despite the presence of HRP activity in the lighter peak (fractions 5–6) as for ssHRP$^{P\text{-}selectin}$. Moreover, secretagogue stimulation did not cause an increase of HRP activity within the light membrane peak, confirming that ssHRP$^{P\text{-}selectinY777A}$ is not sorted to either population of DCG. These data strongly suggest that Tyr777-dependent sorting of HRP–P-selectin chimeras to iDCG occurs at the level of the TGN.

Leu768 within the C1 Domain, as Well as Multiple Determinants within the C2 Domain, Mediate Targeting of HRP–P-Selectin Chimeras to SLMV

Previously, we have demonstrated that HRP–P-selectin chimeras are efficiently transported to SLMV in PC12 cells (Norcott et al., 1996). We have now determined in detail the sequence(s) within the cytoplasmic domain of P-selectin that are needed for trafficking to SLMV, exploiting a glycerol gradient fractionation scheme (Norcott et al., 1996; Clift-O'Grady et al., 1998). We have previously determined that >90% of ssHRP$^{P\text{-}selectin}$ from the SLMV peak on glycerol gradients could be immunoisolated using an antibody to the cytoplasmic domain of p38/synaptophysin (Norcott et al., 1996). Whereas both p38 and ssHRP$^{P\text{-}selectin}$ are present within the SLMV peak on this type of gradient, these fractions are completely devoid of ^{125}I-Trn, thus confirming that the SLMV peak is free from endosomal recycling vesicles (Fig. 5).

After expression of the HRP–P-selectin chimeras in PC12 cells and subcellular fractionation on glycerol gradients, a SLMV targeting index (SLMV-TI) was calculated for each chimera (Fig. 6). Within the C1 domain, substitution of KCPL reduced SLMV targeting by 80% (0.204 ± 0.05) compared with the SLMV-TI of ssHRP$^{P\text{-}selectin}$ (Fig. 6 B). Analysis of single amino acid substitutions across KCPL reveals that replacement of Leu768 with Ala resulted in a similar reduction of SLMV targeting (0.23 ± 0.01) (Fig. 6 C), suggesting that Leu768 within KCPL is required for SLMV targeting. In contrast to the C1 domain, most tetrapeptide substitutions within the C2 domain reduced targeting to SLMV to some degree. In the most dramatic of these, the SLMV-TI for ssHRP$^{P\text{-}selectinYGVF}$ was as low as that for tail-less ssHRP$^{P\text{-}selectin763}$ (SLMV-TI = 0), which was found to accumulate at the plasma membrane (Norcott et al., 1996). Analysis of point mutations within

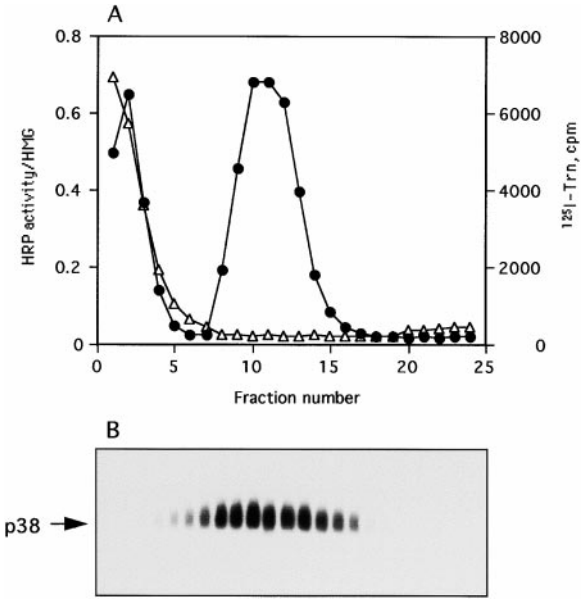

Figure 5. Distribution of HRP activity, ^{125}I-Trn radioactivity and synaptophysin/p38 immunoreactivity after subcellular fractionation on 5–25% Glycerol gradients. (A) PC12 cells expressing wild-type ssHRP$^{P\text{-}selectin}$ were fed with ^{125}I-Trn (△) for 1 h at 37°C, homogenized, and then PNS was fractionated on 5–25% Glycerol gradients to isolate SLMV. HRP activity for ssHRP$^{P\text{-}selectin}$ (●) is expressed in arbitrary units corresponding to the amount of HRP activity in each fraction divided by that in the homogenate. (B) Aliquots from each fraction across the gradient were subjected to 10% SDS-PAGE and Western blotted with polyclonal antibody against p38.

YGVF indicates that Tyr777 makes a major contribution to SLMV targeting and that this residue is tolerant of substitution by another aromatic amino acid (Fig. 6 C) suggesting that, in at least this respect, targeting to both RSO is mediated by the same determinant. Substitution or deletion of DPSP (ssHRP$^{P\text{-}selectinDPSP}$ and ssHRP$^{P\text{-}selectin786}$) reduced SLMV targeting by ~75% (0.25 ± 0.05 and 0.27 ± 0.055, respectively). Altering the sequence between DPSP and YGVF, as seen with ssHRP$^{P\text{-}selectinTNAAF}$, revealed a less severe phenotype (0.43 ± 0.108). Deletions of the C1 or C2 domains, or of the nine carboxy-terminal amino acids (ssHRP$^{P\text{-}selectin\Delta C1}$, ssHRP$^{P\text{-}selectin776}$, and ssHRP$^{P\text{-}selectin782}$, respectively) also dramatically inhibited SLMV targeting (Fig. 6 A).

Lysosomal Targeting of HRP–P-Selectin Chimeras in PC12 Cells

When expressed in several cell lines, including PC12 cells, a substantial proportion of newly synthesized P-selectin is constitutively transported to the plasma membrane and then efficiently endocytosed to lysosomes for degradation (Green et al., 1994; Setiadi et al., 1995; Blagoveshchenskaya et al., 1998a,b; Straley et al., 1998). Findings of cell type–specific variations (Blagoveshchenskaya et al., 1998a,b; Straley et al., 1998) encouraged us to analyze lysosomal targeting in PC12 cells. We have previously established two assays that allow for quantification of lysosomal

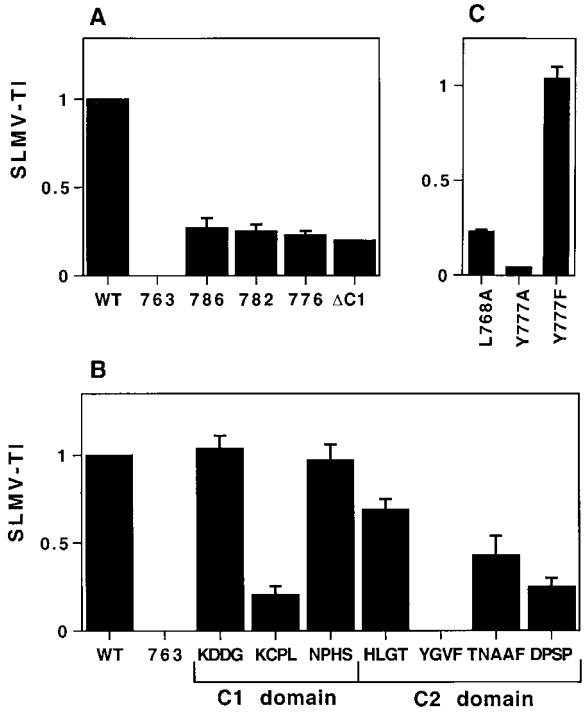

Figure 6. Targeting of HRP–P-selectin chimeras to SLMV in PC12 cells. PC12 cells expressing the HRP–P-selectin chimeras indicated in Fig. 2 were homogenized and fractionated using 5–25% Glycerol gradients to isolate SLMV. SLMV targeting indexes (SLMV-TI) were then calculated. Each bar represents the mean ± SE of 3–10 independent determinations for each chimera. Each SLMV-TI is expressed on a scale related to the WT chimera (SLMV-TI = 1) and the tail-less chimera (SLMV-TI = 0). Deviations of <0.015 are not displayed. (A) SLMV-TIs for the deletion mutants; (B) SLMV-TIs for the tetra-alanine substitutions; (C) SLMV-TIs for the point mutations.

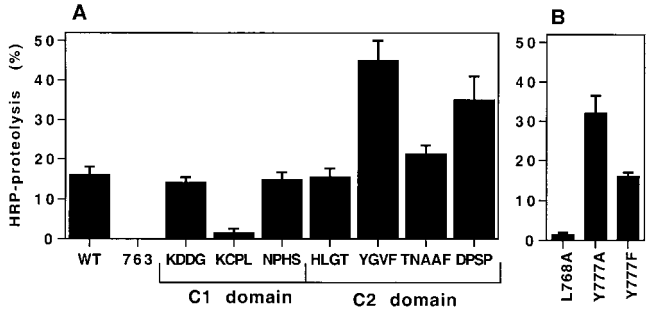

Figure 7. HRP proteolysis of HRP–P-selectin chimeras in PC12 cells. Cells expressing the HRP–P-selectin chimeras indicated were subjected to a Triton X-114 partitioning assay. HRP activity was measured both in the upper hydrophilic phase and in the lower hydrophobic phase to determine the fraction of soluble HRP activity found in the lysate. Each bar represents the mean ± SE of 3–10 independent determinations. (A) The tetra-alanine substitutions; (B) the point mutations.

targeting of HRP chimeras. The first, an HRP proteolysis assay, reveals exposure of chimeras to intracellular proteolytic activity under steady state conditions in living cells. The second assay uses sequential Ficoll velocity gradients for the isolation of lysosomal compartments allowing for calculation of lysosomal targeting indexes (LTI; Blagoveshchenskaya et al., 1998a,b).

As measured by HRP proteolysis, substitution of KCPL within the C1 domain dramatically reduced HRP clipping to 1.43 ± 1.08%, as compared with the average for ssHRP$^{P\text{-selectin}}$ which was 16 ± 2% (Fig. 7 A). Chimeras in which other sequences within the C1 domain have been substituted, i.e., ssHRP$^{P\text{-selectinKDDG}}$ and ssHRP$^{P\text{-selectinNPHS}}$, were proteolyzed as efficiently as ssHRP$^{P\text{-selectin}}$. Analysis of point mutations across KCPL revealed that as for SLMV targeting, Leu768 also operates to promote lysosomal targeting (Fig. 7 B).

In contrast, two mutations of the C2 domain, ssHRP$^{P\text{-selectinYGVF}}$ and ssHRP$^{P\text{-selectinDPSP}}$, exhibited a significant increase in HRP proteolysis, up to 45 ± 5% and 35 ± 6% compared with 16 ± 2% for the wild-type chimera. Tyr777, a critical residue within YGVF for targeting to DCG and SLMV, was also found to be an important residue in preventing lysosomal targeting, since when substituted by Ala but not by Phe, it caused increased HRP clipping of 32 ± 4.4% (Fig. 7 B).

HRP–P-Selectin Chimeras which Are Not Targeted to RSO Are Redirected to Lysosomes via the Plasma Membrane

The analysis of targeting to lysosomes described above was performed under steady state conditions and does not answer the question of whether chimeras pass exclusively via the plasma membrane to lysosomes or are transported directly from the TGN. This is an important point to establish, since a direct route from the TGN to the lysosomes might bypass the compartment from which SLMV bud, thus leading to a misinterpretation of the SLMV targeting data. Therefore, we determined the efficiency of delivery of internalized ^{125}I-2H11 from the plasma membrane to lysosomes using the fractionation procedure designed for isolation of lysosomal compartments.

After a 1-h uptake of ^{125}I-2H11 at 37°C, 11% of ^{125}I-2H11 radioactivity was present in the lysosomal peak of cells expressing ssHRP$^{P\text{-selectin}}$ (Fig. 8 B). However, only 2.8% of the ^{125}I-2H11 intracellular radioactivity was detected in the lysosomal peak from cells expressing ssHRP$^{P\text{-selectin763}}$ (Fig. 8 B). If most ssHRP$^{P\text{-selectin}}$ transfers to lysosomes directly from the TGN, then the amount of ^{125}I-2H11 recovered in the lysosomal peak should have been as low as that for ssHRP$^{P\text{-selectin763}}$ which is clearly not the case. This suggests that the ssHRP$^{P\text{-selectin}}$ that is not sorted to DCG and SLMV is delivered to lysosomes via the plasma membrane. To ascertain whether those chimeras that exhibit the greatest differences in lysosomal targeting also travel via the plasma membrane, we have calculated LTI by ^{125}I-2H11 uptake for each chimera. The LTI for ssHRP$^{P\text{-selectinYGVF}}$ and ssHRP$^{P\text{-selectinDPSP}}$ exceeded those for ssHRP$^{P\text{-selectin}}$ implying that these mutant chimeras are indeed targeted to lysosomes via the plasma membrane (Fig. 8 C). ssHRP$^{P\text{-selectinL768A}}$, which was incapable of targeting to lysosomes, as measured by HRP proteolysis (Fig. 7 B), is not detected in lysosomal fractions as seen by ^{125}I-

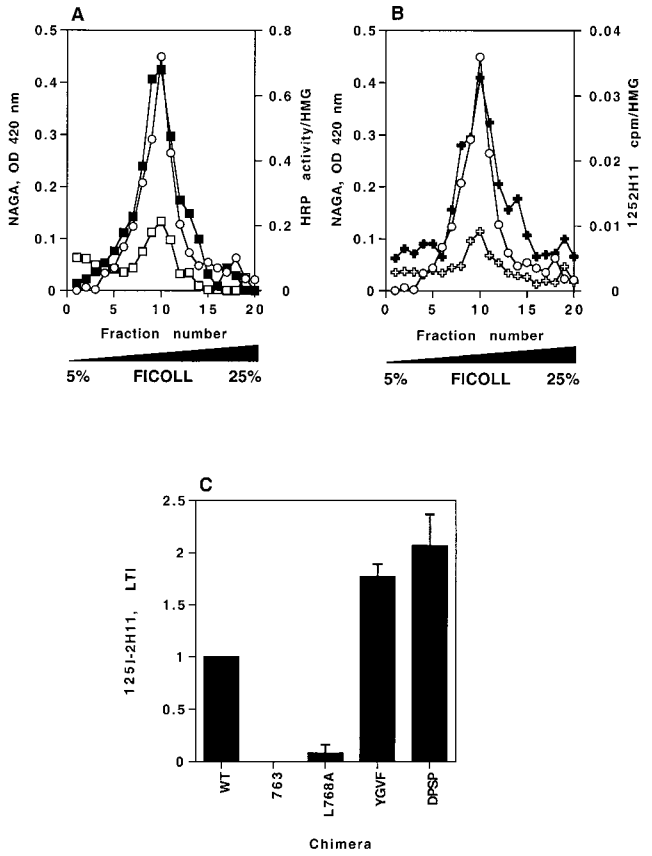

Figure 8. Targeting of internalized ^{125}I-2H11 to lysosomes. PC12 cells expressing the chimeras indicated were fed with ^{125}I-2H11 for 1 h at 37°C and subjected to a two-step fractionation procedure for isolation of lysosomal compartments (see Materials and Methods). A shows the distribution of NAGA (○) compared with HRP activity for ssHRP$^{P\text{-selectin}}$ (■) and tail-less ssHRP$^{P\text{-selectin763}}$ (□). HRP activity was determined in each fraction and normalized to the total HRP activity in the homogenate. B shows the distribution of NAGA activity (○) compared with ^{125}I-2H11 radioactivity for ssHRP$^{P\text{-selectin}}$ (filled plus signs) and for ssHRP$^{P\text{-selectin763}}$ (empty plus signs). ^{125}I-2H11 radioactivity was counted in each fraction across the gradient and normalized to the total radioactivity in the homogenate. (C) the LTI for a variety of chimeras. Each bar represents the mean ± SE of four independent experiments.

2H11 uptake either, indicating that the results obtained by either assay are consistent.

ssHRP$^{P\text{-selectinL768A}}$ Accumulates within ^{125}I-Trn–containing Endosomes

As shown above, Leu768 was found to promote lysosomal targeting of HRP–P-selectin chimeras in PC12 cells. Mutation of this amino acid might act either by blocking exit from the endosomes or by affecting internalization from the plasma membrane. Since the internalization rate for ssHRP$^{P\text{-selectinL768A}}$ is 75% of that of wild-type ssHRP$^{P\text{-selectin}}$ (see Table II), the latter was not the case. To determine whether ssHRP$^{P\text{-selectinL768A}}$ accumulates within Trn-containing endosomes, we have exploited a DAB density shift procedure. DAB cross-linking in the presence of H_2O_2 results in an increase in density of the vulcanized HRP-containing organelles, as seen by subcellular fractionation. PC12 cells transfected so as to transiently express ssHRP-$^{TrnR(tail-)}$ (a chimera between HRP and an amino-terminally truncated TrnR, which is incapable of internalization and therefore accumulates on the plasma membrane, Stinchcombe et al., 1995), ssHRP$^{P\text{-selectin}}$, or ssHRP$^{P\text{-selectinL768A}}$ were analyzed for their ability to shift ^{125}I-Trn using a DAB-reaction protocol. As shown in Fig. 9 and quantitated in Table I, in control cells expressing ssHRP$^{TrnR(tail-)}$ only 8% of the ^{125}I-Trn was shifted (Fig. 9 A). We consider this value to be a basal level, representing signal-independent traffic through the endosomes. It should be noted that DAB shift percentages (Table I) do not measure absolute amounts of chimera within the Trn-containing endosomes since the procedure was performed on transiently expressing cells. They provide comparative data showing differences in the levels of colocalization between different HRP chimeras and ^{125}I-Trn. ssHRP$^{P\text{-selectin}}$ demonstrated higher colocalization with ^{125}I-Trn than ssHRP$^{TrnR(tail-)}$, shifting 13% of the original radioactivity. However, in cells expressing ssHRP$^{P\text{-selectinL768A}}$, the shift was 27%, suggesting that this chimera is concentrated within early Trn-containing endosomes and indicating that Leu768 operates at the level of Trn-positive endosomes to mediate transfer to SLMV and to lysosomes.

DCG, SLMV, and Lysosomal Targeting Determinants Do Not Mediate the Internalization of HRP–P-Selectin Chimeras

Some of the variations in targeting to post-Golgi destinations might be attributable to alterations in internalization rates, as demonstrated for VAMPII (Grote and Kelly, 1996). Therefore, we have measured internalization rates for ssHRP$^{P\text{-selectin}}$, ssHRP$^{P\text{-selectin763}}$, ssHRP$^{P\text{-selectinYGVF}}$, ssHRP$^{P\text{-selectinTNAAF}}$, ssHRP$^{P\text{-selectinDPSP}}$, and ssHRP$^{P\text{-selectinL768A}}$ using a cell surface biotinylation procedure (Blagoveshchenskaya et al., 1998b). First order internalization rates were calculated from data obtained during the first 4 min of endocytosis at 37°C and expressed as %/min (Table II). In agreement with previous studies (Norcott et al., 1996; Blagoveshchenskaya et al., 1998b), ssHRP$^{P\text{-selectin763}}$ was internalized ~10-fold less efficiently than ssHRP$^{P\text{-selectin}}$. Partial inhibition of endocytosis (by 40%) was observed for ssHRP$^{P\text{-selectinDPSP}}$, while the other

Table I. Proportion of HRP–P-Selectin Chimeras Present within ^{125}I-Trn–positive Endosomes

Chimera	% of ^{125}I-Trn radioactivity shifted after DAB reaction	% of DAB shift with background subtracted
ssHRP$^{TrnR(tail-)}$	8	0
ssHRP$^{P\text{-selectin}}$	13	5
ssHRP$^{P\text{-selectinL768A}}$	27	19

PC12 cells expressing the indicated chimera were loaded with ^{125}I-Trn and fractionated on 1–16% Ficoll gradients as described in the legend to Fig. 9. To quantitate the percentage of ^{125}I-Trn shifted after the DAB reaction, the amount of radioactivity remaining in the Trn peak after DAB reaction was divided by the original radioactivity in the endosomal peak in control samples and subtracted from 100%. The extent of DAB shift seen for ssHRP$^{TrnR(tail-)}$ was considered to be a basal level and was subtracted from the values for all the chimeras tested.

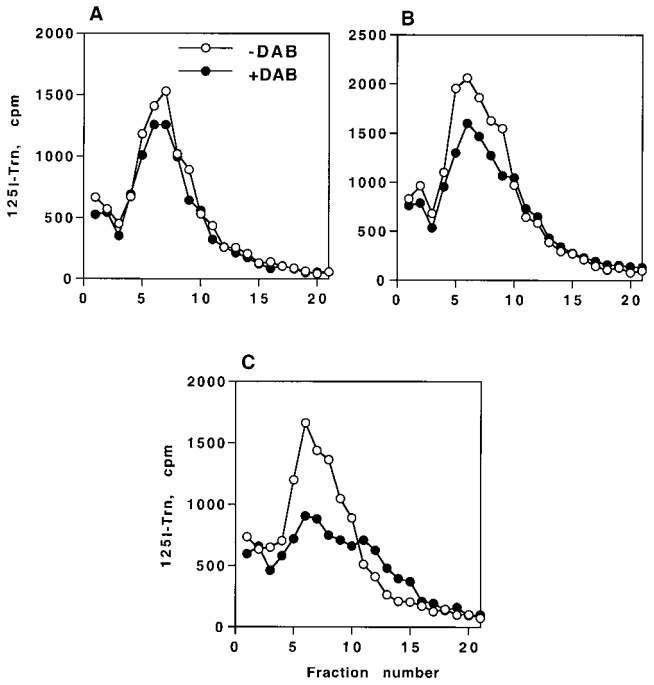

Figure 9. DAB-induced density shift of internalized ^{125}I-Trn in PC12 cells expressing HRP–P-selectin chimeras. Cells expressing ssHRP$^{\text{TrnR(tail}-)}$ (A), ssHRP$^{\text{P-selectin}}$ (B), or ssHRP$^{\text{P-selectinL768A}}$ (C) were fed with ^{125}I-Trn for 60 min at 37°C. Ligand present on the cell surface was removed by MES buffer treatment. Cells were homogenized in HB and the PNS was split into two parts. One half was incubated with DAB and H_2O_2 (●) and the other half with HB alone (○). After the DAB reaction, the samples were centrifuged on 1–16% Ficoll gradients. The distribution of ^{125}I-Trn along these gradients is shown for DAB-incubated or control samples. Data from one typical experiment (out of two) is shown.

chimeras revealed smaller reductions. These data strongly suggest that RSO and lysosomal targeting signals operate independently of internalization from plasma membrane.

Targeting of HRP–P-Selectin Chimeras to SLMV Is a BFA-sensitive Process

Recent data from Shi et al. (1998) have indicated that targeting of VAMPII to SLMV in PC12 cells can occur by two pathways: either directly from the plasma membrane or from endosomes. The former route is thought to be AP2, clathrin, and dynamin dependent and is BFA insensitive, whereas the latter is AP3 and adenosine ribosylation factor (ARF) 1 mediated and is BFA sensitive (Shi et al., 1998). Our data presented above (Figs. 6 and 7) suggest the involvement of an endosomal intermediate en route to SLMV, since both SLMV and lysosomal targeting are dependent on Leu768. To provide further support for this hypothesis, we have examined the BFA sensitivity of SLMV targeting for wild-type HRP$^{\text{P-selectin}}$. Fig. 10 A shows that BFA treatment resulted in an 88% reduction of the HRP activity recovered within the SLMV peak. The magnitude of this effect is similar to the 77% reduction in SLMV targeting found for ssHRP$^{\text{P-selectinL768A}}$ (Fig. 6). This strongly suggests that HRP–P-selectin chimeras

Table II. Initial Internalization Rates of HRP–P-Selectin Chimeras

Chimera	Initial internalization rate
	%/min
ssHRP$^{\text{P-selectin}}$	9.53 ± 0.43
ssHRP$^{\text{P-selectin763}}$	1.01 ± 0.05
ssHRP$^{\text{P-selectinYGVF}}$	7.14 ± 0.31
ssHRP$^{\text{P-selectinTNAAF}}$	7.03 ± 0.40
ssHRP$^{\text{P-selectinDPSP}}$	5.65 ± 0.18
ssHRP$^{\text{P-selectinL768A}}$	7.10 ± 0.20

PC12 cells expressing ssHRP$^{\text{P-selectin}}$, ssHRP$^{\text{P-selectin763}}$, ssHRP$^{\text{P-selectinYGVF}}$, ssHRP$^{\text{P-selectinTNAAF}}$, ssHRP$^{\text{P-selectinDPSP}}$, or ssHRP$^{\text{P-selectinL768A}}$ were biotinylated using NHS-SS-biotin, transferred to 37°C to induce internalization, chilled on ice, and then washed with glutathione to remove any biotin groups remaining on the cell surface. The cells were then lysed, biotinylated proteins were collected on Streptavidin-agarose beads, and then samples were resolved by SDS-PAGE. After transfer to Immobilon-P membranes, the biotinylated HRP–P-selectin chimeras were detected with a polyclonal anti-HRP followed by incubation with ^{125}I–protein A and quantitation by PhosphorImager densitometry. For each chimera, the values are expressed as a percentage of a parallel sample that was kept at 4°C and not treated with glutathione to normalize for the levels of expression.

are passing to SLMV via an endosomal intermediate. As a control, we analyzed levels of the endogenous SLMV membrane protein synaptophysin/p38 in those same SLMV peaks in which HRP activity was measured (Fig. 10 A). As shown in Fig. 10 B, levels of p38 in the SLMV peaks from BFA-treated and untreated cells were identical, confirming the observation of Schmidt et al. (1997) that p38 is sorted to the SLMV from a plasma membrane–derived subcompartment and that this process is therefore BFA insensitive.

Discussion

In this work, we have explored the relationships between trafficking to SLMV, DCG, and lysosomes in PC12 cells, by characterizing the targeting signals of P-selectin, which is localized to all three organelles in this cell line. We have used quantitative measures of the targeting of a series of HRP–P-selectin chimeras to identify the sequences needed for delivery to a variety of destinations. In summary of our results (Fig. 11), we conclude that: (a) While a Tyr-based motif within the cytoplasmic domain is critical for trafficking of HRP–P-selectin to both DCG and SLMV, additional determinants are required to direct this protein to SLMV. (b) There is an overlap between trafficking routes to SLMV and to lysosomes, since Leu768 is essential in exiting from the Trn-positive endosomes for subsequent transfer to either of these organelles. (c) There are complex relationships between targeting to RSO and to lysosomes, since reduction of SLMV or DCG targeting results in a corresponding rise in lysosomal delivery but does not affect delivery to the alternative RSO.

Targeting to Granules

We have discovered that alanine substitution of two short colinear determinants located within the C2 domain of the cytoplasmic tail, YGVF and TNAAF, causes a considerable reduction in targeting to the DCG in PC12 cells. HRP–P-selectin chimeras in which these sequences are substituted by Ala were targeted to DCG at levels only

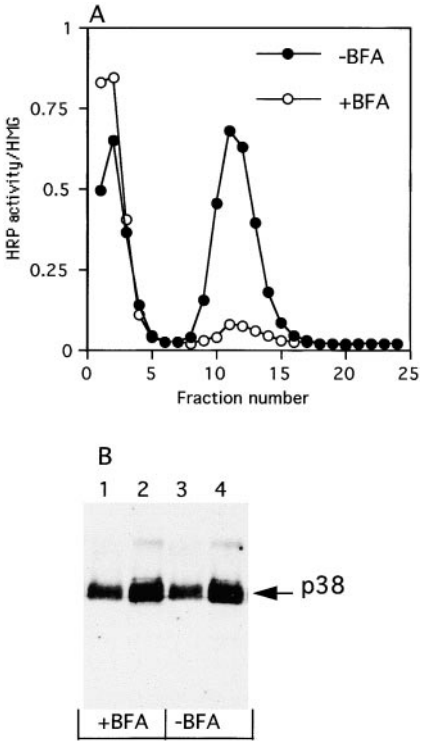

Figure 10. Effect of BFA on the targeting of ssHRP$^{P\text{-selectin}}$ and synaptophysin/p38 to SLMV. (A) PC12 cells expressing ssHRP$^{P\text{-selectin}}$ were incubated in the presence (○) or absence of 10 μg/ml BFA (●) for 1 h at 37°C and a PNS was obtained for centrifugation on 5–25% glycerol gradients. HRP activity was determined in each fraction. Data are expressed as the amount of HRP activity in each fraction divided by that in the homogenate. (B) Aliquots from pooled SLMV peaks, as defined by the distribution of HRP activity shown in A, and from homogenates from the cells treated or mock-treated with BFA were collected, proteins were separated by 10% SDS-PAGE and Western blotted with a polyclonal antibody against p38. Tracks 1 and 3 show p38 in the SLMV peak. Tracks 2 and 4 show p38 in the homogenates. Samples were from the cells treated or mock-treated with BFA, as indicated.

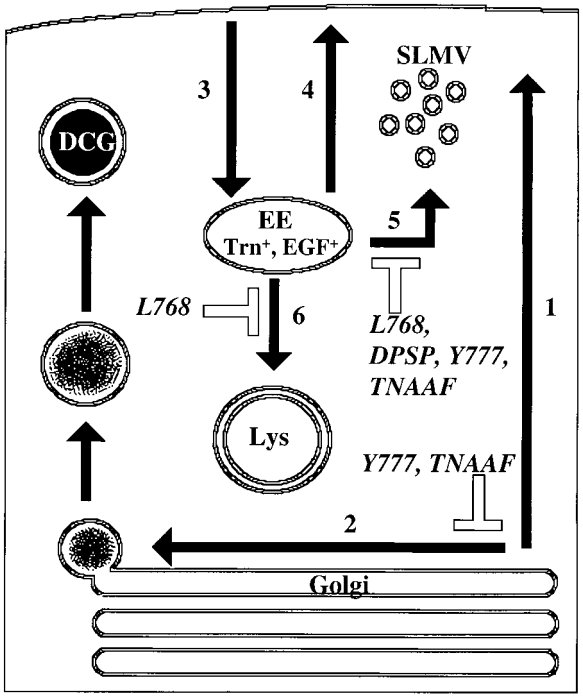

Figure 11. A schematic model for post-Golgi trafficking of P-selectin in PC12 cells. Newly synthesized P-selectin reaching the Golgi is either constitutively transported to the cell surface (1) or is sorted to the DCG in a signal-dependent (*YGVF/TNAAF* with a critical contribution from *Tyr777*) fashion (2). After appearance on the cell surface, it is rapidly internalized into the early, Trn-positive, EGF-positive endosomes (3). From here, some chimera recycles to the plasma membrane (4), whereas the rest is delivered to SLMV (5) or to lysosomes (6). Steps 5 and 6 are mediated by *Leu768*. Trafficking to SLMV (5) from endosomes is also mediated by *Tyr777*, *TNAAF*, and *DPSP*.

10% above that found for the tail-less ssHRP$^{P\text{-selectin763}}$. Analysis of chimeras in which sequences on either side of YGVFTNAAF are deleted shows that removal of the four–amino acid sequence at the carboxy side did not affect DCG targeting. Deleting the C1 domain reduced DCG targeting to basal levels, suggesting that the spacing of YGVF and TNAAF from a lipid bilayer is important for the proper functioning of DCG targeting determinants.

When carboxy-terminal deletions are extended to remove first TNAAF and then both TNAAF and YGVF, we do not find an additive inhibition of DCG targeting, since removal of TNAAF alone (ssHRP$^{P\text{-selectin782}}$) caused the same reduction as removal of YGVFTNAAF (ssHRP$^{P\text{-selectin776}}$). In addition, while TNAAF does not reveal homology to other sorting signals known to promote targeting to different post-Golgi destinations, YGVF is similar to other Tyr-based signals (Trowbridge et al., 1993; Sandoval and Bakke, 1994; Marks et al., 1997). We have found that Tyr777 is important for YGVF to function and is tolerant of conservative replacement with another aromatic amino acid (Fig. 3). Therefore, we speculate that Tyr777 plays a major role within the targeting determinant, while TNAAF may make a local structural contribution to its function.

Our results on identification of DCG targeting determinants within P-selectin partly agree with those obtained in the anterior pituitary line AtT-20 by Modderman et al. (1998). These authors found that Leu768/Asn769 within the C1 domain, as well as Tyr777, Gly778, and Phe780 within the C2 domain, are needed for DCG targeting in AtT-20 cells. Interestingly, the Leu768/Asn769 DCG determinant in AtT-20 cells overlaps with that (Leu768) which functions as a lysosomal targeting signal in both PC12 and NRK cells (this paper and Straley et al., 1998), but has no effect on DCG targeting in PC12 cells. One plausible explanation for this apparent discrepancy is that a recycling route leading to DCG via plasma membrane and endosomal intermediates is more important in AtT-20 than in PC12 cells for maintaining steady state levels of proteins within the granule membrane. If so, then this would explain why mutation of Leu768, which leads to an accumulation of P-selectin within the early Trn-containing endosomes, reduces levels of the protein in the DCG within AtT-20 cells, but not in PC12 cells.

The DCG targeting determinants found in P-selectin do not reveal any homology to the DCG targeting signal identified in VAMPII (Regazzi et al., 1996). Our finding that a Tyr-based sequence promotes DCG targeting was unexpected; Tyr-based motifs are generally thought to be involved in the recruitment of adaptors followed by the binding of clathrin and are therefore concerned with selection for entry into small vesicles. This is difficult to reconcile with a simple model for entry of membrane proteins into forming granules in which sorting in the plane of the membrane precedes budding of an iDCG from the TGN. The role of clathrin and AP1 during subsequent maturation of forming granules is thought to be in the removal via small vesicles of proteins like furin and M6PR that are present in immature but not mature granules (reviewed in Tooze, 1998; Arvan and Castle, 1998). Our data show that the ratio of relative levels of HRP–P-selectin within iDCG (7.2%) and mDCG (14%) is similar to that found for SgII (10 and 28%, respectively). Therefore, we conclude that Tyr 777 promotes sorting to DCG at the level of the TGN since ssHRP$^{\text{P-selectinY777A}}$ was not found in either population of DCG (Fig. 4).

These data lead us to suggest an alternative mechanism used in delivery of membrane proteins to this RSO. We speculate that coats might be involved as planar matrices (Miller et al., 1991) in concentrating proteins within the TGN into "rafts" (microdomains consisting of distinct proteins and lipids found in various membrane compartments; for review see Brown and London, 1998; Thiele and Huttner, 1998; Zegers and Hoekstra, 1998) that could interact with the forming dense core, thus driving granule formation in a process analogous to virus budding. However, until now, this mechanism of sorting at the level of the TGN has only been demonstrated for transmembrane proteins that are involved in apical transport in epithelial cells (Keller and Simons, 1998). A contribution of the transmembrane domain of P-selectin to the formation of DCG (Fleming et al., 1998) would be consistent with the raft model, since the transmembrane domain might facilitate the inclusion of protein within such a raft. Although AP1 and clathrin have not yet been shown to be directly involved in granule formation in the TGN in vivo, in vitro granule budding assays have documented a role for ARF1 (which is implicated in recruitment of AP1 and clathrin to the TGN) in promoting the formation of DCG (Stamnes and Rothman, 1993; Barr and Huttner, 1996; Chen and Shields, 1996). Currently, granule formation is very poorly understood, but a role for cytoplasmic factors, as well as interactions between the core and the lumenal domains of membrane proteins, clearly must be included in models of granule biogenesis.

Targeting to Lysosomes

In this study, we show that KCPL mediates sorting from early Trn-containing endosomes to late endosomes and lysosomes in PC12 cells. Detailed site-directed mutagenesis revealed that Leu768 within this tetrapeptide promotes lysosomal targeting, i.e., operates as a positive lysosomal targeting signal in PC12 cells (Figs. 7 and 8). Substitution of Leu768 caused the retention of this mutant chimera within Trn-positive endosomes as seen by colocalization with ^{125}I-Trn using a DAB-shift procedure (Fig. 9 and Table I).

In addition, some tetra-alanine substitutions within the C2 domain, most notably, YGVF and DPSP, have been found to increase delivery to protease-rich compartments in PC12 cells. This strongly suggests that YGVF and DPSP operate as lysosome avoidance signals at late stages of endocytosis (Figs. 7 and 8), in agreement with results that we obtained previously in H.Ep.2 cells using double mutants (Blagoveshchenskaya et al., 1998b).

Targeting to SLMV

To date, very little is known about the sequences needed for targeting to SLMV. The only protein within which such signals have been characterized in detail is VAMPII, in which an amphipathic α-helix was found to be a necessary requirement for SLMV targeting in PC12 cells (Grote et al., 1995). However, the SLMV targeting signal in VAMPII was later found to be required for endocytosis from plasma membrane implying that internalization and SLMV targeting are controlled by the same signal (Grote and Kelly, 1996). By contrast, our results show that in HRP–P-selectin chimeras, determinants located in both the C1 and C2 domains are implicated in targeting to SLMV regardless of internalization (Fig. 6 and Table II). Within the C1 domain, KCPL and, in particular, Leu768 are necessary requirements for SLMV targeting (Fig. 6). In addition, most sequences within the C2 domain; YGVF (in particular, Tyr777), as well as DPSP and, to a lesser extent, TNAAF, are needed for SLMV targeting (Fig. 6). Thus, the trafficking of HRP–P-selectin chimeras to SLMV is controlled by multiple signals located in different portions of the cytoplasmic tail.

SLMV versus Lysosomal Targeting

An important consideration in understanding SLMV biogenesis is how the signal-mediated trafficking steps en route to SLMV operate with respect to those en route to other post-Golgi destinations, such as lysosomes and DCG. We have discovered that Leu768 is needed for both SLMV and lysosomal targeting. Since substitution of Leu768 leads to an accumulation within early Trn-positive endosomes, exit from this endosomal compartment is not only required for lysosomal targeting but also for delivery to SLMV, implying that SLMV and lysosomal trafficking involve the same endosomal intermediate. In contrast, mutations of sequences within the C2 domain, i.e., YGVF, TNAAF, and DPSP, block SLMV targeting, but also cause an increase in targeting to lysosomal compartments, as judged by subcellular fractionation and HRP proteolysis (Figs. 7 and 8). Thus there is clearly a signal-dependent trafficking choice between endosomes, lysosomes and SLMV.

SLMV Formation Involves an Endosomal Intermediate for HRP–P-Selectin Chimeras

Currently, there is evidence for two possible routes taken by membrane proteins targeted to SLMV: (a) direct budding from the plasma membrane (or an elaboration thereof) (Takei et al., 1996; Schmidt et al., 1997; Murthy

and Stevens, 1998) and (b) via an endosomal intermediate (Clift-O'Grady et al., 1990; Norcott et al., 1996; Lichtenstein et al., 1998). The former route was found to be adaptor complex AP2, clathrin, and dynamin dependent (Takei et al., 1996; Shupliakov et al., 1997), while the latter is temperature sensitive (Desnos et al., 1995) and ARF1 (Faundez et al., 1997) and adaptor complex AP3 dependent (Faundez et al., 1998). However, it may well be that the two pathways can coexist in the same cell (Koenig and Ikeda, 1996; Shi et al., 1998).

The results described in this paper support the view that the delivery of P-selectin to the SLMV proceeds via an endosomal intermediate which is Trn-positive and is most likely analogous to that observed by Lichtenstein et al. (1998), since failure to exit from this compartment, as exemplified by ssHRP$^{\text{P-selectinL768A}}$, also impairs delivery to the SLMV. Studies from Faundez et al. (1997) and Shi et al. (1998) suggest that generation of SLMV from endosomal intermediates is BFA sensitive, whereas the direct formation of SLMV from the plasma membrane is not (Shi et al., 1998). We have now demonstrated that SLMV targeting of HRP–P-selectin chimeras is inhibited by BFA (Fig. 10 A), which reduces the SLMV-TI to the level of ssHRP$^{\text{P-selectinL768A}}$ in untreated cells (Fig. 6). In contrast, SLMV targeting of an endogenous membrane marker protein, synaptophysin/p38, is not affected by BFA (Fig. 10 B), indicating that this protein may be delivered to SLMV directly from the plasma membrane in agreement with Schmidt et al. (1997). Extending the finding of two routes taken by one protein to SLMV (Shi et al., 1998), our results strongly suggest that different SLMV proteins may preferentially use one of the two alternative pathways. Whether this choice is dependent on the presence of any particular SLMV targeting signal remains to be investigated.

Structural Requirements for Targeting to DCG and SLMV Overlap, but Are Not Identical

Despite the established phenomenon of dual localization of membrane proteins to both RSO (Schmidle et al., 1991; Walch-Solimena et al., 1993; Chilcote et al., 1995; Papini et al., 1995; Regazzi et al., 1996), the targeting requirements needed to achieve this biorganellar distribution have not been analyzed in detail. We have found that YGVF and TNAAF are necessary for the targeting of P-selectin both to SLMV and to DCG. However, in both cases mutation of TNAAF caused a smaller reduction of targeting to either RSO compared with that of YGVF with its critical Tyr777. We would therefore argue that YGVF engages with the sorting machinery, while TNAAF operates as a contextual requirement within which YGVF functions. Nevertheless, these data show that the same determinants are needed for delivery to both RSO. Consistent with our data, a similar observation was previously documented for VAMPII, in which a point mutation within the amphipathic α-helix abrogated targeting of this protein to both insulin-containing secretory granules and SLMV in pancreatic β cells (Regazzi et al., 1996). These findings of a common targeting requirement for sorting to RSO may not be fortuitous. First, despite their different origin, both RSO are involved in stimulation-induced release of neurotransmitters followed by fusion with the same acceptor membrane, the plasma membrane, and exo-endocytic recycling, i.e., they do share aspects of their itinerary. Second, a common targeting requirement may account for the secretagogue-dependent transfer of membrane proteins from one RSO to the other (Strasser et al., 1999, in press). Third, the two major classes of sorting signals, tyrosine-based and dileucine motifs, have both been documented to operate at more than one location in the cell (Höning et al., 1995, 1996; Hunziker and Geuze, 1996).

We have also shown that the substitution of a sequence centered on Leu768, as well as of DPSP, abolished targeting to SLMV but did not affect targeting to DCG (Figs. 3 and 6). The existence of these additional sequences needed to target proteins to SLMV presumably reflects the differences in biogenesis of the two RSO: while DCG are formed from the TGN, SLMV biogenesis involves the constitutive delivery of SLMV proteins to the cell surface before they are sorted away to the final destination (Regnier-Vigouroux et al., 1991; Arvan and Castle, 1998). Altogether, these data suggest that whereas targeting to both RSO is mediated by a common signal, additional determinants are required for progression of P-selectin through endosomal intermediates en route to SLMV (see above).

An Overview of the P-Selectin Itinerary

In this paper, we describe for the first time the sequence-dependent triorganellar targeting within one cell line for a single protein. We have summarized our data in a diagram (Fig. 11). Our data are consistent with a view of traffic as flowing along the secretory pathway to the TGN, at which point a proportion of HRP–P-selectin chimera is selected for incorporation into iDCG; a process mediated by a Tyr-based sorting signal. This P-selectin then remains within granules as they are modified into mDCG. The remainder passes to the cell surface and internalizes into the early Trn-positive endosomes before passing along the endocytic pathway towards the lysosomes or to the SLMV. Exit from the Trn-positive endosome requires Leu768. En route to the lysosome some proportion of P-selectin is diverted into SLMV in a DPSP and/or Tyr777-dependent fashion.

The effects of mutagenesis as described above are predictable within such a scheme. Thus, impairment of SLMV or DCG targeting, as revealed by ssHRP$^{\text{P-selectinDPSP}}$ or ssHRP$^{\text{P-selectinY777A}}$, leads to an increase in lysosomal targeting, whereas knockout of SLMV and lysosomal targeting, as seen for ssHRP$^{\text{P-selectinL768A}}$, results in retaining of the chimera in Trn-positive endosomes.

Another important aspect of our findings is of the relative contribution of different pathways to each destination. We have shown that a recycling route operating via the Trn-positive endosome does not make a significant contribution to steady state levels of ssHRP$^{\text{P-selectin}}$ in DCG. This conclusion comes from the observation that accumulation in Trn-positive endosomes of ssHRP$^{\text{P-selectinL768A}}$, which would otherwise reach SLMV and lysosomes, does not affect targeting to DCG. These findings suggest that a direct route into granules at the level of the TGN is likely to play the major role in controlling steady state levels of P-selectin in DCG in these cells. By contrast, our finding that

Leu768, which mediates exit from Trn-positive endosomes, plus sequences within the C2 domain that modulate lysosomal trafficking are both required for SLMV targeting provide evidence that the endosomal route makes the major contribution in delivery of P-selectin to SLMV. Finally, our data delineating the relationships between the different post-Golgi pathways clearly indicates a hierarchy of trafficking choices operating to direct P-selectin to its multiple destinations.

We would like to thank Dr. M. Arribas for a critical review of the manuscript.

This work was supported by a Wellcome Trust International Travelling Fellowship to A.D. Blagoveshchenskaya and by Medical Research Council support for A.D. Blagoveshchenskaya, E.W. Hewitt, and D.F. Cutler.

Received for publication 27 January 1999 and in revised form 25 May 1999.

References

Arvan, P., and D. Castle. 1998. Sorting and storage during secretory granule biogenesis: looking backward and looking forward. *Biochem. J.* 332:593–610.

Barr, F.A., and W.B. Huttner. 1996. A role for ADP-ribosylation factor 1, but not COP I, in secretory vesicles biogenesis from the trans-Golgi network. *FEBS Lett.* 384:65–70.

Bauerfeind, R., and W.B. Huttner. 1993. Biogenesis of constitutive secretory vesicles, secretory granules and synaptic vesicles. *Curr. Opin. Cell Biol.* 5:628–635.

Blagoveshchenskaya, A.D., J.P. Norcott, and D.F. Cutler. 1998a. Lysosomal targeting of P-selectin is mediated by a novel sequence within its cytoplasmic tail. *J. Biol. Chem.* 273:2729–2737.

Blagoveshchenskaya, A.D., E.W. Hewitt, and D.F. Cutler. 1998b. A balance of opposing signals within the cytoplasmic tail controls the lysosomal targeting of P-selectin. *J. Biol. Chem.* 273:27896–27903.

Bonfanti, R., B.C. Furie, B. Furie, and D.D. Wagner. 1989. PADGEM (GMP-140) is a component of Weibel-Palade bodies of human endothelial cells. *Blood.* 73:1109–1112.

Brown, D.A., and E. London. 1998. Functions of lipid rafts in biological membranes. *Annu. Rev. Cell Biol.* 14:111–136.

Chen, Y.G., and D. Shields. 1996. ADP-ribosylation factor-1 stimulates formation of nascent secretory vesicles from the trans-Golgi network of endocrine cells. *J. Biol. Chem.* 271:5297–5300.

Chilcote, T.J., T. Galli, O. Mundigl, L. Edelmann, P.S. McPherson, K. Takei, and P. DeCamilli. 1995. Cellubrevin and synaptobrevins: similar subcellular localization and biochemical properties in PC12 cells. *J. Cell Biol.* 129:219–231.

Clift-O'Grady, L., A.D. Linstedt, A.W. Lowe, E. Grote, and R.B. Kelly. 1990. Biogenesis of synaptic vesicles-like structures in a pheochromocytoma cell line PC12. *J. Cell Biol.* 110:1693–1703.

Clift-O'Grady, L., C. Desnos, Y. Lichtenstein, V. Faundez, J.-T. Horng, and R.B. Kelly. 1998. Reconstitution of synaptic vesicle biogenesis from PC12 cell membranes. *Methods (Orlando).* 16:150–159.

Connolly, C.N., C.E. Futter, A. Gibson, C.R. Hopkins, and D.F. Cutler. 1994. Transport into and out of the Golgi complex studied by transfecting cells with cDNAs encoding horseradish peroxidase. *J. Cell Biol.* 127:641–647.

Cramer, L.P., and D.F. Cutler. 1992. Sorting between secretory pathways. *In* Protein Traffic: A Practical Approach. A. Masterson and T. Wileman, editors. Oxford University Press, New York. 57–85.

Cutler, D.F., and L.P. Cramer. 1990. Sorting during transport to the surface of PC12 cells: divergence of synaptic vesicles and secretory granule proteins. *J. Cell Biol.* 110:721–730.

Desnos, C., L. Clift-O'Grady, and R.B. Kelly. 1995. Biogenesis of synaptic vesicles in vitro. *J. Cell Biol.* 130:1041–1049.

Disdier, M., J.H. Morrisey, R.D. Fugate, D.F. Bainton, and R.P. McEver. 1992. Cytoplasmic domain of P-selectin (CD 62) contains the signal for sorting into the regulated secretory pathway. *Mol. Biol. Cell.* 3:309–321.

Dittie, A.S., L. Thomas, G. Thomas, and S.A. Tooze. 1997. Interaction of furin in immature secretory granules from neuroendocrine cells with the AP-1 adaptor complex is modulated by casein kinase II phosphorylation. *EMBO (Eur. Mol. Biol. Organ.) J.* 16:4859–4870.

Elferink, L.A., M.R. Peterson, and R.H. Scheller. 1993. A role for synaptotagmin (p65) in regulated exocytosis. *Cell.* 72:153–159.

Faundez, V., J.-T. Horng, and R.B. Kelly. 1997. ARF1 is required for synaptic vesicles budding in PC12 cells. *J. Cell Biol.* 138:505–515.

Faundez, V., J.-T. Horng, and R.B. Kelly. 1998. A function for the AP3 coat complex in synaptic vesicle formation from endosomes. *Cell.* 93:423–432.

Fleming, J.C., G. Berger, J. Guichard, E.M. Cramer, and D.D. Wagner. 1998. The transmembrane domain enhances granular targeting of P-selectin. *Eur. J. Cell Biol.* 75:331–343.

Green, S.A., H. Setiadi, R.P. McEver, and R.B. Kelly. 1994. The cytoplasmic domain of P-selectin contains a sorting determinant that mediates rapid degradation in lysosomes. *J. Cell Biol.* 124:435–448.

Grote, E., and R.B. Kelly. 1996. Endocytosis of VAMPII is facilitated by a synaptic vesicle targeting signal. *J. Cell Biol.* 132:537–547.

Grote, E., J.C. Hao, M.K. Bennet, and R.B. Kelly. 1995. A targeting signal in VAMP regulating transport to synaptic vesicles. *Cell.* 81:581–589.

Höning, S., and W. Hunziker. 1995. Cytoplasmic determinants involved in direct lysosomal sorting, endocytosis, and basolateral targeting of rat lgp120 (lamp-I) in MDCK cells. *J. Cell Biol.* 128:321–332.

Höning, S., J. Griffith, H.J. Geuze, and W. Hunziker. 1996. The tyrosine-based lysosomal targeting signal in lamp-1 mediates sorting into Golgi-derived clathrin-coated vesicles. *EMBO (Eur. Mol. Biol. Organ.) J.* 15:5230–5239.

Hunziker, W., and H.J. Geuze. 1996. Intracellular trafficking of lysosomal membrane proteins. *Bioessays.* 18:379–389.

Johnston, G.I., R.G. Cook, and R.P. McEver. 1989. Cloning of GMP-140, a granular membrane protein of platelets and endothelium: sequence similarity to proteins involved in cell adhesion and inflammation. *Cell.* 56:1033–1044.

Keller, P., and K. Simons. 1998. Cholesterol is required for surface transport of influenza hemagglutinin. *J. Cell Biol.* 140:1357–1367.

Koedam, J.A., E.M. Cramer, E. Briend, B. Furie, B.C. Furie, and D.D. Wagner. 1992. P-selectin, a granular membrane protein of platelets and endothelial cells, follows the regulated secretory pathway in AtT-20 cells. *J. Cell Biol.* 116:617–625.

Koenig, J.H., and K. Ikeda. 1996. Synaptic vesicles have two distinct recycling pathways. *J. Cell Biol.* 135:797–808.

Kornfeld, S., and I. Mellman. 1989. The biogenesis of lysosomes. *Annu. Rev. Cell Biol.* 5:483–525.

Kornilova, E.S., D. Taverna, W. Hoeck, and N.E. Hynes. 1992. Surface expression of erbB-2 protein is post-transcriptionally regulated in mammary epithelial cells by epidermal growth factor and by the culture density. *Oncogene.* 7:511–519.

Larsen, E., A. Celi, G.E. Gilbert, B.C. Furie, J.K. Erban, R. Bonfanti, and B. Furie. 1989. PADGEM protein: a receptor that mediates the interaction of activated platelets with neutrophils and monocytes. *Cell.* 59:305–312.

Lichtenstein, Y., C. Desnos, V. Faundez, R.B. Kelly, and L. Clift-O'Grady. 1998. Vesiculation and sorting from PC12-derived endosomes *in vitro*. *Proc. Natl. Acad. Sci. USA.* 95:11223–11228.

Marks, M.S., H. Ohno, T. Kirchhausen, and J.S. Bonifacino. 1997. Protein sorting by tyrosine-based signals: adapting to the Ys and wherefores. *Trends Cell Biol.* 7:124–128.

McEver, R.P., J.H. Beckstead, K.L. Moore, L. Marshall-Carlson, and D.F. Bainton. 1989. GMP-140, a platelet α-granule membrane protein, is also synthesized by vascuolar endothelial cells and is localized in Weibel-Palade bodies. *J. Clin. Invest.* 84:92–99.

Miller, K., M. Shipman, I.S. Trowbridge, and C.R. Hopkins. 1991. Transferrin receptors promote the formation of clathrin lattices. *Cell.* 65:621–632.

Modderman, P.W., E.A. Beuling, L.A. Govers, J. Calafat, H. Janssen, A.E. Von dem Borne, and A. Sonnenberg. 1998. Determinants in the cytoplasmic domain of P-selectin required for sorting to secretory granules. *Biochem. J.* 336:153–161.

Murthy, V.N., and C.F. Stevens. 1998. Synaptic vesicles retain their identity through the endocytic cycle. *Nature.* 392:497–501.

Norcott, J.P., R. Solari, and D.F. Cutler. 1996. Targeting of P-selectin to two regulated secretory organelles in PC12 cells. *J. Cell Biol.* 134:1229–1240.

Papini, E., O. Rosetto, and D.F. Cutler. 1995. VAMP-2 is associated with dense-core secretory granules in PC12 neuroendocrine cells. *J. Biol. Chem.* 270:1332–1336.

Partoens, P., D. Slembrouck, J. Quatacker, P. Baudhuin, P.J. Courtoy, and W.P. De Potter. 1998. Retrieved constituents of large dense-cored vesicles and synaptic vesicles intermix in stimulation-induced early endosomes of noradrenergic neurons. *J. Cell Sci.* 111:681–689.

Patzak, A., and H. Winkler. 1986. Exocytotic exposure and recycling of membrane antigens of chromaffin granules: ultrastructural evaluation after immunolabeling. *J. Cell Biol.* 102:510–515.

Regazzi, R., K. Sadoul, P. Meda, R.B. Kelly, P.A. Halban, and C.B. Wollheim. 1996. Mutational analysis of VAMP domains implicated in Ca^{2+}-induced insulin exocytosis. *EMBO (Eur. Mol. Biol. Organ.) J.* 15:6951–6959.

Regnier-Vigouroux, A., S.A. Tooze, and W.B. Huttner. 1991. Newly synthesized synaptophysin is transported to synaptic-like microvesicles via constitutive secretory vesicles and the plasma membrane. *EMBO (Eur. Mol. Biol. Organ.) J.* 10:3589–3601.

Sandoval, I.V., and O. Bakke. 1994. Targeting of membrane proteins to endosomes and lysosomes. *Trends Cell Biol.* 4:292–297.

Schmidle, T., R. Weiler, C. Desnos, D. Scherman, R. Fischer-Colbrie, E. Floor, and H. Winkler. 1991. Synaptin/synaptophysin, p65 and SV2: their presence in adrenal chromaffin granules and sympathetic large dense core vesicles. *Biochim. Biophys. Acta.* 1060:251–256.

Schmidt, A., M.J. Hannah, and W.B. Huttner. 1997. Synaptic-like microvesicles of neuroendocrine cells originate from a novel compartment that is continuous with the plasma membrane and devoid of transferrin receptor. *J. Cell Biol.* 137:445–458.

Setiadi, H., M. Disdier, S.A. Green, W.M. Canfield, and R.P. McEver. 1995. Residues throughout the cytoplasmic domain affect the internalization of P-selectin. *J. Biol. Chem.* 270:26818–26826.

Shi, G., V. Faundez, J. Roos, E.C. Dell'Angelica, and R.B. Kelly. 1998. Neuroendocrine synaptic vesicles are formed in vitro by both clathrin-dependent and clathrin-independent pathways. *J. Cell Biol.* 143:947–955.

Shupliakov, O., P. Low, D. Grabs, H. Gad, H. Chen, C. David, K. Takei, P. De Camilli, and L. Brodin. 1997. Synaptic vesicles endocytosis impaired by disruption of dynamin-SH3 domain interactions. *Science*. 276:259–263.

Stamnes, M.A., and J.E. Rothman. 1993. The binding of AP-1 clathrin adaptor particles to Golgi membranes requires ADP-ribosylation factor, a small GTP-binding protein. *Cell*. 73:999–1005.

Stinchcombe, J.C., H. Nomoto, D.F. Cutler, and C.R. Hopkins. 1995. Anterograde and retrograde traffic between the rough endoplasmic reticulum and the Golgi complex. *J. Cell Biol.* 131:1387–1401.

Straley, K.S., B.L. Daugherty, S.E. Aeder, A.L. Hockenson, K. Kim, and S.A. Green. 1998. An atypical sorting determinant in the cytoplasmic domain of P-selectin mediates endosomal sorting. *Mol. Biol. Cell*. 9:1683–1694.

Strasser, J.E., M. Arribas, A. Blagoveshchenskaya, and D.F. Cutler. 1999. Secretagogue-triggered transfer of membrane proteins from neuroendocrine secretory granules to synaptic-like microvesicles. *Mol. Biol. Cell.* In press.

Subramaniam, M., J.A. Koedam, and D.D. Wagner. 1993. Divergent fates of P- and E-selectins after their expression on the plasma membrane. *Mol. Biol. Cell*. 4:791–801.

Subtil, A., M. Delepierre, and A. Dautry-Varsat. 1997. An α-helical signal in the cytosolic domain of the interleukin 2 receptor beta chain mediates sorting towards degradation after endocytosis. *J. Cell Biol.* 136:583–595.

Takei, K., O. Mundigl, L. Daniell, and P. De Camilli. 1996. The synaptic vesicle cycle: a single vesicle budding step involving clathrin and dynamin. *J. Cell Biol.* 133:1237–1250.

Thiele, C., and W.B. Huttner. 1998. Protein and lipid sorting from the trans-Golgi network to secretory granules—recent developments. *Semin. Cell Biol.* 9:511–516.

Tooze, S.A. 1998. Biogenesis of secretory granules in the trans-Golgi network of neuroendocrine and endocrine cells. *Biochim. Biophys. Acta.* 1404:231–244.

Tooze, S.A., and W.B. Huttner. 1990. Cell-free protein sorting to the regulated and constitutive secretory pathways. *Cell.* 60:837–847.

Tooze, S.A., T. Flatmark, J. Tooze, and W.B. Huttner. 1991. Characterization of the immature secretory granule, an intermediate in granule biogenesis. *J. Cell Biol.* 115:1491–1503.

Trowbridge, I.S., J.F. Collawn, and C.R. Hopkins. 1993. Signal-dependent membrane protein trafficking in the endocytic pathway. *Annu. Rev. Cell Biol.* 9:129–161.

von Grafenstein, H., and D.E. Knight. 1992. Membrane recapture and early triggered secretion from the newly formed endocytic compartment in bovine chromaffin cells. *J. Physiol. Lond.* 453:15–31.

Walch-Solimena, C., K. Takei, K.L. Marek, K. Midyett, T.C. Sudhof, P. De-Camilli, and R. Jahn. 1993. Synaptotagmin: a membrane constituent of neuropeptide-containing large dense-core vesicles. *J. Neurosci.* 13:3895–3903.

Wiley, H.S., and D.D. Cunningham. 1982. The endocytic rate constant. A cellular parameter for quantitating receptor-mediated endocytosis. *J. Biol. Chem.* 257:4222–4229.

Zegers, M.M.P., and D. Hoekstra. 1998. Mechanisms and functional features of polarized membrane traffic in epithelial and hepatic cells. *Biochemistry J.* 236:257–269.